Journal of Superconductivity: Incorporating Novel Magnetism, Vol. 14, No. 6, December 2001 (© 2001)

Study of Atomic Motions in $EuBa_2Cu_3O_{7-\delta}$ by Mössbauer and EXAFS Spectroscopies

F. Piazza,[1] E. Abraham,[1] L. Cianchi,[2] F. Del Giallo,[2] G. Spina,[3] F. Allegretti,[3] and P. Ghigna[4]

Received and accepted 15 August 2001

We report the results of ^{151}Eu Mössbauer and Eu K-edge EXAFS measurements on samples of $EuBa_2Cu_3O_{7-\delta}$. In particular, the ratios between the Eu Debye–Waller factors along the *c* and *ab*-plane directions, were obtained from the Mössbauer spectra in the temperature range 10–300 K. From these ratios, we obtained the differences between the corresponding mean square displacements. Moreover the motions of the first four coordination shells of the europium with respect to the latter, for $T = 30$–300 K, were studied by means of EXAFS spectroscopy. Combining the results obtained with the two techniques, we construct a qualitative picture of the collective atomic motions. In particular, we identify a substructure in the unit cell, around the central ion, formed by atoms performing correlate large amplitude anharmonic oscillations.

KEY WORDS: high-T_c superconductivity; atomic motions; Mössbauer; EXAFS.

1. INTRODUCTION

Many of the models that have been proposed in order to establish the nature of high-T_c superconductivity involve unusual vibrational properties of the cuprates [1]. However, despite the large number of experimental and theoretical studies performed on cuprate lattice dynamics, many important questions have not yet been clarified. One of these questions concerns the existence of large anharmonicities in the atomic motions, which is invoked in many experimental and theoretical works on high-T_c superconductivity [2–7]. On the other hand, for the recently discovered superconducting MgB_2, a combined *ab initio calculation* and neutron scattering study has revealed that huge anharmonic oscillations of the boron atoms are strongly coupled to the electron in states near the Fermi surface [8].

In a previous work, we performed a very accurate measure of the mean square displacement (MSD) of the europium in $EuBa_2Cu_3O_7$ by means of ^{151}Eu Mössbauer spectroscopy [9]. The Debye–Waller factor was determined as a function of the temperature by using the absolute absorption area method (*only by this method low-temperature anarmonicities can be revealed* [10]). We found that the Eu MSDs were about four times greater than the values expected for usual harmonic oscillation.

Obviously, the Eu compound is not anomalous, i.e., the properties of the RBCO compounds are largely independent of the trivalent R ion (except for R = Pr or La). We then expect that the oscillatory amplitude of the R ion is approximately the same irrespective of R, except small differences due to the different ionic radii and masses.

In Ref. [9] Mössbauer spectra were taken on powder sample with randomly-oriented EBCO grains, so that the MSDs obtained should be the average values of the MSDs in the *c* and *ab*-plane directions. Here, a comparison between the MSDs in

[1]Physics Department, Heriot-Watt University, Edinburg EH14 4AS, United Kingdom.
[2]Istituto di Fisica Applicata – CNR, 50127 Firenze, Italy.
[3]Physics Department, University of Florence, 50019 Sesto F.no, Firenze, Italy.
[4]Chemistry–Physics Department, University of Pavia, 27100 Pavia, Italy.

0896-1107/01/1200-0675/0

these two directions will be performed by measuring the f_c/f_{ab} ratio between the Debye–Waller factors. Moreover, we present EXAFS measurements of the mean square relative displacement (MSRD) of the first atomic coordination shells of the Eu ion. As a consequence, from Mössbauer and EXAFS data, we were able to extract information on single-atom motions and correlations among these motions.

2. MÖSSBAUER EXPERIMENT

In the region of linear absorption, the absorption Mössbauer area A for a single line spectrum is given by $A = f_s \alpha t_a$, where $t_a = m_a f_a \sigma_0$ is the so-called effective thickness, m_a is the mass of the Mössbauer isotope per unit area of the sample, f_s and f_a are the f-factors of source and sample, respectively. Lastly, α is a constant that depends on the natural line width Γ_n and line hyperfine broadening.

Since the unit cell has quasi-tetragonal symmetry, we will assume the (a, b) MSD of the europium to be isotropic, but different from the MSD in c direction: $\langle x_{ab}^2 \rangle \neq \langle x_c^2 \rangle$. Under this assumption f_a depends only on the angle θ between the γ-ray k vector and the c-axis. By posing $\langle x^2 \rangle = \langle x_c^2 \rangle \cos^2(\theta) + \langle x_{ab}^2 \rangle \sin^2(\theta)$, we can write $f_a(\theta) = f_{ab} r^{\cos^2(\theta)}$, where $r = f_c/f_{ab}$. Thus, if $p(\theta)$ denotes the distribution function of the grain orientation in the sample, the absorption Mössbauer area is given by

$$A = f_s \alpha m_a \sigma_0 f_{ab} \int_0^\pi p(\theta)\, r^{\cos^2(\theta)}\, \sin(\theta)\, d\theta \qquad (1)$$

In order to measure the ratio r, the absorption areas of two sample with different grain-orientation distributions $p_1(\theta)$ and $p_2(\theta)$ have to be compared. To do this, we considered the quantity $Z_{12} = (A_1/m_1)/(A2/m_2)$, which, for Eq. (1), is given by

$$Z_{12} = \frac{\int_0^\pi p_1(\theta)\, r^{\cos^2(\theta)}\, \sin(\theta)\, d\theta}{\int_0^\pi p_2(\theta)\, r^{\cos^2(\theta)}\, \sin(\theta)\, d\theta} \qquad (2)$$

In this equation, the ratio r is implicitly expressed in terms of Z_{12}. Therefore, the r value can be obtained from the numerical analysis of Eq. (2), when $p_1(\theta)$, $p_2(\theta)$, and Z_{12} have been determined.

2.1. Mössbauer Samples

Two samples (samples 1 and 2) of oriented single-phase powder of $EuBa_2Cu_3O_7$ (purity 99.9% and mean grain size 2 μm) and a sample of randomly-oriented, single-phase powder (sample 3) of $EuBa_2Cu_3O_7$ were prepared, all in the form of flat disks. The orientation was obtained by means of two different methods: we mixed the powder with epoxy resin and shaped it in a 8-T magnetic field directed along the holder axis. The mixture was kept within the field at a temperature of -10°C for about 1 h so as to prevent the glue from hardening during the grain orientation. The temperature was then increased to about 25°C and kept at this value, in the presence of the field, for the time required to make the glue solid (about 0.5 h). Since the magnetic susceptibility of EBCO has the maximum component perpendicular to the c-axis [11–14], the grains of EBCO orient themselves with the c-axis perpendicular to the field, i.e. parallel to the sample surface.

Another oriented-grain sample, but with the c-axis mainly directed perpendicular to the faces, was obtained by exerting a pressure of about 10 MPa on a mixture of powders of EBCO and polythene for 1 day. The micrograins of EBCO have a laminar shape; therefore, the pressure tends to orient the *lamellae* perpendicularly to the force [13–16].

Finally, a randomly-oriented grain sample was obtained by preparing a mixture of EBCO powder and epoxy resin and letting the glue harden in the absence of orienting forces.

All our samples were made with medium thickness so as to avoid the presence of holes, which would have compromised a correct estimate of the Mössbauer absorption areas. Therefore, correction due to saturation of the spectra is expected to be necessary.

2.2. Mössbauer Results

A detailed description of the determination of the sample masses and orientation degrees is reported elsewhere [17]. Here, we just say that masses were obtained from the absorption measurement of the radiations of 14.4 and 122 keV emitted from a ^{57}Co source. Moreover, the orientation distribution functions were obtained by X-ray diffraction. Bragg spectra were collected using the CoK_α emission.

Conventional Mössbauer transmission measurements were performed by using a 100 mCi source of ^{151}Sm in SmF_3. For each sample, spectra at the temperatures of 20, 85, 90, 95, 200, and 300 K were collected. Cooling was achieved by means of a Gifford-Mac Mahon cryogenerator [18], and the temperature was stabilized by an ITC4 *Oxford Instrument* controller. In order to determine the non-Mössbauer background

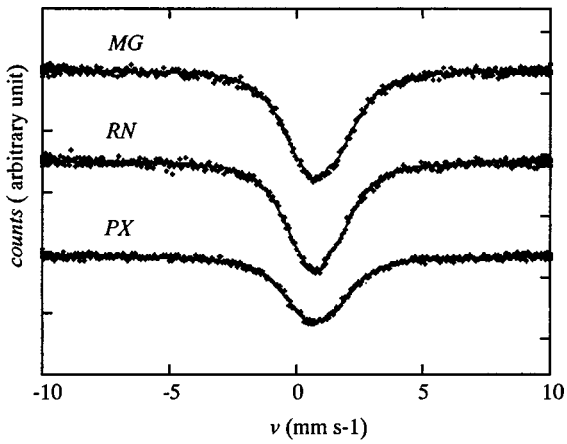

Fig. 1. Mössbauer spectra of the three samples at $T = 20$ K and relative fits. Count scales are the same for the three spectra; the baselines are shifted.

fraction N_B/N_∞, PHA spectra were also collected for each sample and for each temperature [17]. If A_M is the area given back by the fitting procedure of a Mössbauer spectrum, the Mössbauer absorption area A is given by $A = A_M/(1 - N_B/N_\infty)$. Finally, in order to obtained the Z-ratios, absorption areas were corrected taking into account saturation effects, according to the procedure described in detail in [17]. Mössbauer spectra at 20 K, together with their fits, are reported as example in Fig. 1, where MG, PX, and RN denote samples with grains oriented by magnetic field, by pressure, and randomly, respectively.

The f_c/f_{ab} ratios at the temperatures considered are reported in Fig. 2. They were evaluated from the Z-values corresponding to the sample couples MG–RN, PX–RN, and MG–PX.

We see that the f-factor of the ^{151}Eu in EBCO is strongly anisotropic. The ratio $r = f_c/f_{ab}$ turned

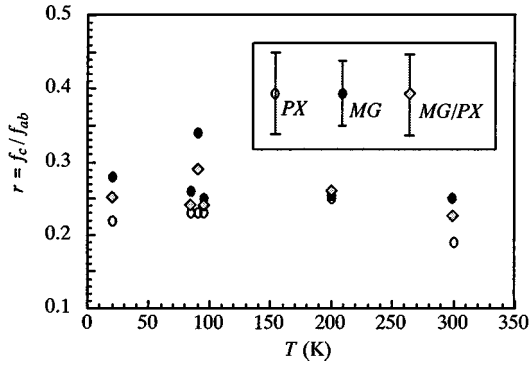

Fig. 2. r values corresponding to the MG–RN, PX–RN, and MG–PX data couples. The error bars, which are independent of the temperature, are shown in the window.

out to be practically independent of the temperature and its value is around 0.25, with a statistical error of about 0.05. By denoting with $\langle x_c^2 \rangle$ and $\langle x_{ab}^2 \rangle$ the mean square displacements of the europium ion in the c-direction and in the ab-planes, respectively, and with k the wave vector of the 21.6 keV Mössbauer γ-rays, i.e. $k = 10.93$ Å^{-1}, we have

$$\langle x_c^2 \rangle - \langle x_{ab}^2 \rangle = -\frac{\ln(r)}{k^2} = (1.2 \pm 0.2) \times 10^{-2} \text{ Å}^2 \quad (3)$$

This very large value agrees with a previous Mössbauer result [9] in proving the presence of a low-temperature vibrational anharmonicity of the europium motion. Moreover, the present work shows that this anharmonicity mainly affects the motion along c-direction.

By assuming for $\langle x_{ab}^2 \rangle$ the value of 0.003 Å^2, which was obtained for yttrium in the compound $YBa_2Cu_3O_{6.98}$ in the temperature range $T = 45$–90 K [19], we obtain $u_c = \sqrt{\langle x_c^2 \rangle} \approx 0.12$ Å. So large a low-temperature oscillation amplitude means that the europium potential has not a parabolic shape along c. Rather, it has to have a flat or wine-bottle-like bottom, whose width is about 0.1 Å.

3. EXAFS EXPERIMENT

As mentioned in the Introduction, EXAFS measurements were performed for investigating the mean square variations of the distances of the atoms from europium; therefore, non-oriented-grain samples could be used. On the other hand, a tetragonal nonsuperconducting sample and an orthorombic sample were prepared in order to reveal possible differences in the relative motions of the atoms. To be precise, we prepared two samples of $EuBa_2Cu_3O_{7-\delta}$ single-phase powders mixed with polyethylene, with $\delta \approx 1$ and $\delta \approx 0$ ($T_c \approx 90$ K). For each of them, we collected transmission Eu K-edge EXAFS spectra at $T = 30$, 60, 90, 120, 180, 250, and 300 K. The measurements were performed at the beam-line GILDA CRG of the European Synchrotron Radiation Facility (ESRF) in Grenoble. We carried out the data analysis by fitting the experimental spectra with the aid of the GNXAS package [20].

The model cluster used for the EXAFS calculations is shown in Fig. 3, which represents the local structure around Eu in EuBCO up to a radial distance R_0 of 4 Å. The four shells included in the calculations are denoted as Eu—O, Eu—Cu, Eu—Ba, and Eu—Eu(2), in order of (their) increasing distance

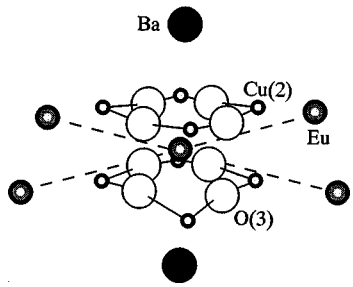

Fig. 3. Cluster used in the simulation of the EXAFS spectra. In order of increasing distance from the Eu site, one can see the O shell, the Cu shell, the Ba shell, and the shell of Eu's lying in the adjacent cells.

from Eu. Actually, the EXAFS Fourier transform (FT) shows further components above 4 Å, but their analysis is much less accurate. Therefore, they have not been considered in fitting the experimental data.

In order to determine the signal shape, only single scattering of the four coordination spheres was considered, as the contributions of the multiple scattering paths (MSPs) were verified to be negligible. This is because a large part of MSPs have lengths much larger than $2R_0$, so that the corresponding signal amplitudes are much smaller than the simple scattering ones. Moreover, the MSPs with lengths shorter than $2R_0$ correspond to double scattering paths with angles different from zero, i.e. with small scattering amplitudes. We assumed the Gaussian approximation of the radial-distribution function. The centers R and the line widths σ of its peaks represent the mean values and the standard deviations of the coordination-sphere radii, respectively.

The validity of Gaussian approximation was checked by fitting the spectra including the cumulants C_3 and C_4. The values obtained for C_2 $(=\sigma^2)$ were equal, within the permissible errors, to the ones obtained with the position $C_3 = C_4 = 0$. We accounted for two different subcoordination shells for each neighbor. On the contrary, only one σ^2 was enough to obtain good fits of the spectra.

Apart from this the coordination spheres were divided in two subspheres with one half of atoms each, but with different R's and the same σ's.

The S_0^2 parameter accounting for multielectronic excitations was kept free only in the preliminary fits. The values obtained for this parameter showed no dependence on the doping level δ and temperature. Therefore, in the last fits S_0^2 was set at the value of 0.85, i.e., the average of the values obtained in the preliminary fits.

In order to determine the signals corresponding to the various scattering paths, we used the Heding–Lundqvist potential that allows to do an *ab initio* evaluation of the signal-amplitude decrease due to anelastic scatterings. Therefore, it was not necessary to introduce the photoelectron mean free path as free parameter.

3.1. EXAFS Results

A typical EXAFS signal with corresponding FT is shown in Fig. 4. We can distinguish three different regions. In the region from 4 to 6 $Å^{-1}$, the small amplitude oscillations are mainly due to scattering from the oxygen atoms of the first coordination shell. In fact the oxygen atom backscattering amplitude has

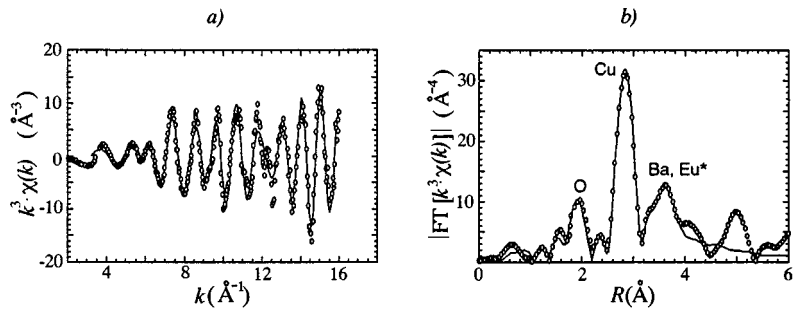

Fig. 4. (a) Eu K-edge EXAFS signal measured in the underdoped sample at a representative temperature $T = 30$ K multiplied by k^3. Circles are experimental points. The solid line is the result of the fit. (b) Magnitude of the FT of the representative signal shown beside. Small circles: experimental. Solid line: fit. The fit of the signal for $k \approx 12$ $Å^{-1}$ is less accurate. This is because the contribution to the spectra for $k \approx 12$ $Å^{-1}$ comes from the remote shells, which are not taken into account in our signal calculation.

Table I. EXAFS-MSRDs for the Underdoped EBCO

T (K)	σ^2_O (10^{-3} Å^2)	σ^2_{Cu} (10^{-3} Å^2)	σ^2_{Ba} (10^{-3} Å^2)	σ^2_{Eu} (10^{-3} Å^2)
30	4.0 (5)	2.1 (2)	3.0 (6)	2.2 (3)
60	4.1 (5)	2.2 (2)	3.5 (7)	2.2 (3)
90	4.4 (5)	2.5 (2)	3.9 (8)	2.4 (3)
120	4.7 (6)	2.9 (2)	4.1 (9)	3.2 (4)
180	5.5 (7)	3.7 (3)	4.6 (10)	4.2 (5)
250	6.7 (9)	4.7 (3)	5.5 (16)	5.1 (8)
300	8.1 (11)	5.2 (4)	7.4 (19)	6.0 (10)

significant values only in this region, where the contribution of the other shells is negligible. In the central region (6–11 Å^{-1}) the signal is mainly due to scattering from the second-shell copper atoms, though here contributions from barium and europium external shells are present. However the latter contributes to the signal mainly for k larger than 11 Å^{-1}.

The fitting of the signal FT shows that we have a rather good agreement for the first three peaks, which correspond to the considered for coordination shells. The peaks of the barium and europium shells are not spatially resolved because their shell radii, $R_3 = 3.7$ Å and $R_4 = 3.9$ Å, respectively, are very close. As R increases, the agreement between FT_{exp} and FT_{th} becomes worse. For instance, the small hump on the right side of the Eu–Ba peak, around $r \approx 4$ Å, which is due to single scattering from the fifth and sixth shells, was not included in our model.

As far as the structural parameters are concerned, we found that the average distances between europium and its neighbors do not vary appreciably (less than 0.5% for temperature up to 300 K). The trend of the MSRDs are more interesting. The best fit values are reported, together with their statistical errors, in Tables I and II for the samples with $\delta \approx 0$ and $\delta \approx 1$, respectively. It can be seen that they lie in a range which is consistent with normal harmonic vibration (see, e.g., [21], where the σ^2 values for copper are reported). Moreover, the σ^2's of the first two shells do not depend on the doping. On the contrary, the σ_i^2's corresponding to the Ba and Eu(2) shells are observed to be somewhat smaller for the overdoped sample.

Table II. EXAFS-MSRDs for the Overdoped EBCO

T (K)	σ^2_O (10^{-3} Å^2)	σ^2_{Cu} (10^{-3} Å^2)	σ^2_{Ba} (10^{-3} Å^2)	σ^2_{Eu} (10^{-3} Å^2)
30	4.2 (7)	2.0 (2)	1.4 (4)	1.3 (3)
60	4.2 (7)	2.0 (2)	1.4 (4)	1.3 (3)
90	4.4 (8)	2.5 (2)	2.4 (6)	1.6 (3)
120	4.7 (8)	2.8 (2)	2.7 (7)	2.3 (8)
180	5.3 (10)	3.4 (3)	2.8 (9)	3.2 (12)
250	6.8 (12)	4.8 (3)	4.4 (14)	5.3 (18)
300	7.5 (12)	5.2 (4)	4.8 (12)	5.7 (16)

4. CORRELATIONS AMONG IONIC MOTIONS

As is well known, the EXAFS Debye–Waller factors measure the broadening of the bond distances because of the thermal motions, provided the static disorder is negligible. Denoting by σ_1^2 and σ_2^2 the absorber and the backscatterer MSDs along the interatomic distance R_{12}, respectively, the corresponding σ^2_{EXAFS} can be written as

$$\sigma^2_{EXAFS} = \sigma_1^2 + \sigma_2^2 - 2\rho_{12}\sigma_1\sigma_2 \qquad (4)$$

where ρ_{12} is the so-called correlation parameter. If $\rho_{12} \approx \pm 1$, the motion is highly correlated, in-phase or out-of-phase, respectively. If $\rho_{12} \approx 0$, the ionic oscillations are uncorrelated. Generally, a decrease of $|\rho_{12}|$ is expected as the interatomic distance increases. Furthermore, if the Debye model is a good approximation for the considered solid, ρ_{12} is expected to be an increasing function of temperature. This is a consequence of the correlations, as seen by EXAFS, being projected onto the absorber–backscatterer bond distance, thereby being 1D correlations in their very nature [22].

Some qualitative conclusions regarding the correlations among ion motions can be drawn here as follows. Let us consider the ionic radii of Eu^{3+} and O^{2-}. We see that the two ions are practically in contact with each other.[5] Consequently, a large positive correlation between the motions of the europium and oxygen ions of the first shell is expected. Moreover, taking into account the tight binding between the oxygen and copper ions in the CuO_2 planes, a large positive correlation is also expected with the copper ions of the second shell [23]. On the other hand, we note that Ba^{2+} ions are not in contact with the inner shells. Nevertheless, the corresponding measured σ^2 seems to be rather small. Then, in order for these results to be consistent with the large oscillation of the Eu ion along $\hat{c}$, as measured by Mössbauer spectroscopy, a large positive correlation between the two ions has to exist. As a side result, we can combine the Mössbauer value for the σ^2_{Eu} in the

[5] Values of 1.4 and 1.08 Å are reported for O^{2-} and Eu^{3+} ions respectively. They add up to 2.48 Å, when the Eu−O distance is 2.41 Å from our measurements and in good agreement with the crystallographic data. http://www.webelements.com.

$(\hat{a}, \hat{b})$ plane with the σ^2_{EXAFS} to calculate ρ_{Eu-Eu} as a function of temperature. Unlike the normal trend, ρ_{Eu-Eu} decreases monotonically from $\approx$1 to $\approx$0.75 as the temperature increases from 30 to 300 K.

5. CONCLUSIONS

By combining the Mössbauer and EXAFS results we suggest that the ionic motions in EBCO consist of large-amplitude, highly-correlated oscillations with superimposed small-amplitude, weakly-correlated vibrations. The large-amplitude component can be described as follows. Starting from the equilibrium configuration, let us imagine we displace the Eu ion along $\hat{c}$. As a consequence, the oxygen ions will move along the line joining the Eu and O centers (see Fig. 5). But this displacement hardly changes the Eu—O distance, and therefore, it will not be revealed by EXAFS. Hence, the measured σ^2_{Eu-O}'s correspond only to the small-amplitude component. The same considerations apply to the Cu ions, since their motions are closely correlated with the motions of the oxygen neighbors [23].

The rather small values of σ^2_{Eu-Ba} measured in our experiment may seem surprising. In fact, since Ba^{2+} ions are not in contact with the inner shells, the large-amplitude oscillations of Eu along $\hat{c}$, as measured by Mössbauer spectroscopy, would result in a large-amplitude relative motion for these two ions. However, σ^2_{Eu-Ba}'s are fairly small. Consequently, we should conclude that the motions of barium and europium are strongly and positively correlated despite their rather large separation. A possible explanation could be that because of coulomb interaction between the Eu^{3+} and Ba^{2+} ions, when the former moves in a certain direction the latter is forced to move in the same direction, and *vice versa*. We also note that the large displacements of the oxygen ions result in a variation of the sum of their attractive forces on the barium ions. This in turn increases the correlation between europium and barium motions. To summarize, the large anharmonic oscillation includes the Eu and Ba motions along $\hat{c}$ and the rotation around the cell center of the oxygen ions of the first shell.

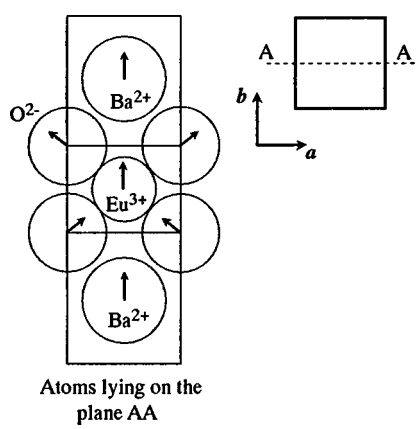

Fig. 5. Schematic representation of the O and Ba shells in an EBCO unit cell drawn to scale. The arrows represent large displacements of the ions, which are caused by a large displacement of the europium ion along $\hat{c}$.

Finally, we observe that our experiments do not reveal remarkable differences between the underdoped and overdoped samples. The σ^2_{Eu-O} and σ^2_{Eu-Cu} values clearly show that the relative motions of these ions are independent of the doping level. On the contrary, the σ^2_{Eu-Ba} and σ^2_{Eu-Eu} values of the overdoped sample are significantly smaller than those of the underdoped one at $T < T_c$. Such a difference could be due to the coupling phenomenon that takes place at $T < T_c$ in the superconducting sample. However, in order to clarify this question, further investigations will be necessary. We also note that the observed decrease in ρ_{Eu-Eu} as the temperature increases cannot be explained within the framework of phonon theory.

REFERENCES

1. D. Mikailovic, G. Ruani, E. Kaldis, and K. A. Müller, eds., in *Proceedings of the International Workshop on Anharmonic Properties of High-Tc Cuprates.* (World Scientific, Singapore, 1995).
2. J. Mustre de Leon, S. D. Conradson, I. Batistić, and A. R. Bishop, *Phys. Rev. Lett.* **65,** 1675 (1990).
3. A. Bianconi, M. Lusignoli, N. L. Saini, P. Bordet, A. Kvick, and P. G. Radaelli, *Phys. Rev. B* **54,** 4310 (1996).
4. A. Bussmann-Holder and A. R. Bishop, *Phys. Rev. B* **56,** 5297 (1997).
5. F. Cordero, R. Cantelli, M. Corti, A. Campana, and A. Rigamonti, *Phys. Rev. B* **59,** 12078 (1999).
6. R. P. Sharma, S. B. Ogale, Z. H. Zhang, J. R. Liu, W. K. Chu, B. Veal, A. Paulikas, H. Zheng, and T. Venkatesan, *Nature* **404,** 736 (2000).
7. A. Bussmann-Holder, K. A. Müller, R. Micnas, H. Büttner, A. R. Bishop, and T. Egami, *J. Phys.: Condens. Matter* **13,** L169 (2001).
8. T. Yildirim, O. Gülseren, J. W. Lynn, C. M. Brown, T. J. Udovic, Q. Huang, N. Rogado, K. A. Regan, M. A. Hayward, J. S. Slusky, T. He, M. K. Haas, P. Halifah, K. Inumaru, and R. J. Cava, *Phys. Rev. B* **87,** 037001 (2001).
9. M. Capaccioli, L. Cianchi, F. Del Giallo, F. Pieralli, and G. Spina, *J. Phys.: Condens. Matter* **7,** 2429 (1995).
10. B. Kolk, *Studies of Dynamical Properties of Solids With the Mössbauer Effect, Vol. 5* (North-Holland, Amsterdam, 1984), pp. 1–328.
11. D. B. Knorr and J. D. Livingston, *Supercond. Sci. Technol.* **1,** 302 (1989).

12. L. Duran, F. Kircher, P. Régnier, D. Chateigner, N. Pellerin, F. J. Gotor, P. Simon, and P. Odier, *Supercond. Sci. Technol.* **8,** 214 (1995).
13. R. Eggenhöffner, A. Tuccio, R. Masini, A. Diaspro, S. Leporatti, and R. Rolandi, *Supercond. Sci. Technol.* **10,** 142 (1997).
14. D. E. Farrel, B. S. Chandrasekar, M. R. D. Guire, M. M. Fang, V. G. Kogan, J. R. Clem, and D. K. Finnemore, *Phys. Rev. B* **36,** 4025 (1987).
15. G. Desgarding, I. Monot, and B. Raveau, *Supercond. Sci. Technol.* **12,** R115 (1999).
16. J. R. Thompson, D. K. Christen, S. T. Sekula, B. C. Sales, and L. A. Boatner, *Phys. Rev. B* **36,** 836 (1987).
17. L. Cianchi, F. Del Giallo, F. Lucchi, and G. Spina, *Hyper. Int.* **3,** 4 (2001).
18. A. Baldini, F. Cecconi, F. Del Giallo, F. Pieralli, and G. Spina, *Nucl. Instr. Meth. B* **62,** 549 (1992).
19. P. Schweiss, W. Reichardt, M. Braden, G. Collin, G. Heger, H. Claus, and A. Erb, *Phys. Rev. B* **49,** 1387 (1994).
20. A. Filipponi and A. Di Cicco, http://gnxas.unicam.it (1996).
21. R. B. Greegor and F. W. Lytle, *Phys. Rev. B* **20,** 4902 (1979).
22. G. Beni and P. M. Platzman, *Phys. Rev. B* **14,** 1514 (1976).
23. A. Lanzara, N. L. Saini, A. Bianconi, F. Duc, and P. Bordet, *Phys. Rev. B* **59,** 3851 (1999).